CHAPTER 58

ON THE OVERLAND FLOW OF TSUNAMI AND EFFECTIVENESS OF WALL AS A COUNTER MEASURE

Toshio Iwasaki
Professor of Tohoku University
and
Hiroyoshi Togashi
Assistant of Tohoku University

Tohoku University Sendai, Japan

SYNOPS1S

When a tsunami of large magnitude strikes a coast line, various kinds of disaster such as loss of lives, properties or public investments are caused by inundation of tsunami over nearly horizontal area. Although tsunami runup has been investigated for the sloping beach, these populated area is bordered on sea by a vertical wall such as a quaywail or a highway revetment. In this paper, transformation of tsunami waves at a vertical quaywall is analysed using U-C characteristics and overland flow is treated. Effectiveness of a vertical land dike aiming to stop running water is investigated also. Theoretical results are verified by experiments.

1NTRODUCT1ON

Tsunami is caused by a mid-ocean earthquake of large magnitude, having very flat steepness, very long wavelength of several hundred kilometers and wave period of several ten minutes in the ocean. When it approaches to a coast, wave height is increased by effect of shallowness as understood easily by the Green's theorem. Moreover tsunami is amplified by diffraction and reflection owing to favorable nearshore topography and also by harbour resonance. As a result, several or several ten meters of wave height is not unusual which results catastrophic disaster.

In Japan, 101 tsunamis have been recorded since 687, in which 18 tsunamis caused catastrophe. Sanriku Coast is situated in northern part of Honshu, the main island of Japan and faced to the Pacific seismic belt, so this coast has been attacked by tsunamis most frequently in Japan. As this coast is a rias type, there are various kinds of bays in their scale and shape, which depth is usually over 10 or 20 meters at their mouth and have vertical cliffs on most of coastline leaving scarce flat land at the innermost part, where fishery ports and harbours are located with populated area behind it. Stepping over quaywalls of ports and harbours or highway revetments, tsunami waves cause overland flow. Although tsunami runup on a sloping beach has been investigated extensively by various authors, overland flow of this type seems a problem to be solved still now.

This paper deals with mechanism of transformation of tsunami wave at a quaywall and that of overland flow and effectiveness of a land dike as a counter measure.

U-C CHARACTERISTICS OF LONG WAVES OF FINITE AMPLITUDE

As long waves of finite amplitude, following relationships hold also for tsunam1 waves,

for C+ characteristics
$$P=c_{x}2(C-1)+U$$
 (1)

for C- characteristics
$$Q=c_{\star}2(C-1)-U$$
 (2)

in which analysis is confined to one dimensional and the slope of the sea bottom is assumed horizontal. $c*is\sqrt{gh}$, $C=(1+\eta/h)^{1/2}$ and U=u/c*where h is the depth, g is the acceleration of the gravity and u is the horizontal velocity. (Lamb 1932)

Eq. (1) implies a U-C characteristics in a U-C plane corresponding to a C+ characteristics in a X-T plane has negative slope of 1/2 which intersects the horizontal axis at a point $(P/c_*, 0)$ which is shown in fig.1. Also by eq. (2), a U-C characteristics corresponding to a C- characteristics has positive slope of 1/2 which intersects the horizontal axis at a point $(-Q/c_*, 0)$

In the progressive wave, Q=0. Hence $U_1=2(C_1-1)$, $P/c_{\overline{x}}4(C_1-1)$ and this is expressed by a point A, namely A₁, A₂, A₃ or A_p corresponding to their value of P/c_* or $4(C_1-1)$ which can be determined by 7 or surface elevation of each wave element, where suffix 1 refers to values of incident waves and suffix p refers to values at the peak. When these wave elements are stopped at the vertical quaywall, U=0. So, point A moves to point B, namely B_1 , B_2 , B3 or Bp which shows U-C characteristics of a perfect clapotis. Then,

$$Cc-1=2(C_1-1) \tag{3}$$

clopotis.

The reflected wave elements can be expressed by points c_1 , c_2 , c_3 and c_p as these characteristics must pass points B and $v_r=-2(c_r-1)$ since P=0, where suffix r refers to a reflected wave.

When C_1-1 is larger than $1/2(C_w-1)$, overruning flow takes place, where $C_{W}\!\!=\!\!(1\!+\!\frac{H_{W}}{h})^{1/2}$ in which H_{W} is the quaywall height above still water. the clapotis at the quaywall is imperfect. Assumption is made for these reflected wave elements that the velocity is same with incident wave elements, but the surface elevation cannot be higher than h+Hw, or Cr-1=1/2. $(C_{w}-1)$.

Then Cc-1 can be given by two characteristics through C, and Cr as shown in fig.2. So,

$$C_{c}-1=\frac{3}{2}(C_{1}-1)+\frac{1}{4}(C_{w}-1)$$
 (4)

$$U_{c}=(C_{1}-1)-\frac{1}{2}(C_{w}-1)$$
 (5)

Where C_w-1 is smaller than $2(C_1-1)$. That is,

$$C_{w}-1 < 2(C_{1}-1)$$
 (6)

It may seem interest that when water level is equal to the height of the quaywall, reflection is took place only as time sequence of the velocity without wave configuration as shown in fig.3. In this case,

$$C_{c}-1=3/2(C_{1}-1) \tag{7}$$

and

$$U_{c}=C_{1}-1 \tag{8}$$

as C_w -1=0. And since U_c and C_c -1 are positive, these wave elements invade into land causing overland flow.

OVERLAND FLOW OF TSUNAMI

Experiments show that when overland flow was occured, water depth decreased abruptly at the brink of the quaywall as shown in fig.4 and flow was assumed being transformed from subcritical to supercritical.

For overland flow no-dimensional wave celerity is defined as

$$C' = \sqrt{\frac{\eta'}{h}} \tag{9}$$

Where η' is measured from the horizontal bed. Then since

$$\eta_{c}' = \eta_{c}^{-H}$$
 (10)

$$C_{c}^{\dagger} = \sqrt{\frac{\eta_{c} - H_{w}}{h}} = \sqrt{C_{c}^{2} - C_{w}^{2}}$$
 (11)

As Uc'=Uc, the following relation can be obtained.

$$C_c^{12} - U_c^{2} = 5/16 J^2 + 3/2 JC_w$$
 (12)

in which

$$J = 2C_1 - C_w - 1 \tag{13}$$

Since J is positive when overrunning is occured, the right hand side of eq.(12) is positive which means C_c ' is larger than U_c ', or flow is subcritical at the brink of the quaywall.

Then a critical flow section A is assumed established at some distance from the brink followed by supercritical flow. As this distance has not been decided yet, an assumption is made here that this distance is infinitely small and the section of critical flow is situated just next to the brink of the quaywall.

For calculation of overrunning flow, the origin of x-axis is taken at the brink of the quaywall. C_+ characteristics emerging from t-axis are expressed by

$$\frac{\mathrm{d}\mathbf{x}}{\mathrm{d}\mathbf{t}} = \mathbf{U}_{\mathbf{c}}' + \mathbf{C}_{\mathbf{c}}' \tag{14}$$

and on which

$$U_{c}' + 2C_{c}' = U_{A}' + 2C_{A}'$$
 (15)

As mentioned above,

$$U_{\mathbf{A}}' = C_{\mathbf{A}}' \tag{16}$$

Then from (15) and (16)

$$U_{A}' = C_{A}' = 1/3(U_{C}' + 2C_{C}') \tag{17}$$

, in which $\rm U_c$ '= $\rm U_c$ and $\rm C_c$ ' are given already. As the distance between 0 and A is infinitely small, the two points are coincided practically and are considered to give a boundary condition.

C- characteristics emerging from A-axis are given by,

$$\frac{\mathrm{d}\mathbf{x}}{\mathrm{d}\mathbf{t}} = \mathbf{U}_{\mathbf{A}}' - \mathbf{C}_{\mathbf{A}}' = 0 \tag{18}$$

, which shows C- characteristics are parallel with t-axis and range of influence is limited to the right half of x-t plane as accepted in practice.

Overrunning flow is resembled with flow after the breaking of a dam in which various assumptions has been presented for the front condition. According to the theory originally proposed by St. Venant, the front depth is zero and so C_+ and C_- characteristics coincide with each other to compose the characteristic envelope. However a more general relation is

$$C_{\mathbf{f}}' = \mathbf{a} U_{\mathbf{f}}' \tag{19}$$

for the front condition, in which a is a constant and a reciprocal of the Froude number and suffix f refers to the front. (Abbot, 1961) (Méhauté, 1964) Then the characteristic equation for the leading wave element is,

$$d(U'+2C') = -f\left(\frac{U'}{C'}\right)^2 \frac{dx}{U'+C'}, \tag{20}$$

in which f is a friction coefficient and X=x/h. From eq. (20),

$$\frac{U^{12}}{2} = \frac{U_A^{12}}{2} - \frac{f}{a^2} \cdot \frac{X - X_A}{(1+a)(1+2a)}$$
 (21)

for the horizontal bed after Freeman and Méhauté. The front is the envolope of the leading wave element given by

$$\frac{dX}{dT} = U' \tag{22}$$

Eliminating U' from eq. (21) and (22), the leading front characteristics are given.

As shown in fig.5, the succeeding C_+ characteristics emerging from a point F takes over the leading front emerging from a point E. Then on the C_- characteristics,

$$\mathbf{U}_{\mathbf{f}}^{'} + 2\mathbf{C}_{\mathbf{f}}^{'} = \mathbf{U}_{\mathbf{F}}^{'} + 2\mathbf{C}_{\mathbf{F}}^{'} - \mathbf{f} \left(\frac{\mathbf{U}_{\mathbf{F}}^{'}}{\mathbf{C}_{\mathbf{F}}^{'}}\right)^{2} \cdot \Delta \mathbf{T}_{\mathbf{F}\mathbf{G}}$$
(23)

and on the leading front

$$C_{f} = aU_{f}$$
 (24)

Then from eq. (23) and (24)

$$C_{\mathbf{f}}' = \frac{\mathbf{a}}{1+2\mathbf{a}} \cdot \left[\mathbf{U}_{\mathbf{F}}' + 2C_{\mathbf{F}}' - \mathbf{f} \left(\frac{\mathbf{U}_{\mathbf{F}}'}{C_{\mathbf{F}}'} \right)^2 \cdot \Delta \mathbf{T}_{\mathbf{F}G} \right]$$
 (25)

and also

$$U_{f}' = \frac{1}{1+2a} \left[U_{F}' + 2C_{F}' - f \left(\frac{U_{F}'}{C_{F}'} \right)^{2} \cdot \Delta T_{FG} \right]$$
 (26)

After this intersection G, velocities are changed in accordance with eq. (21) until a next C_+ characteristics takes over.

Internal zone bounded by the t-axis and the characteristic envelope of the leading front can be analysed by two sets of characteristics as

Froude number of the leading front or 1/a is normally assumed as 2 from works by Keulegan, Abbott, Méhauté and others.

REFLECTION AND OVERFLOW AT THE LAND DIKE

Along the Sanriku coast, many land dikes have been constructed to protect resident quarters as one of counter measures for running water of tsunami. Although their height was designed in accordance with the highest trace of inundation, its reliability has not been checked until tsunamis struck these areas by chile earthquake in 1960 which stimulated us beginning this research.

Fig.6 shows schematically reflection and overflow of running tsunami at a land dike. As the Froude number of the leading front is assumed as 2, the incident flow is supercritical in section I. So a bore is occured by reflection, behind which flow is subcritical. If the height of a land dike is lower than that of the reflected bore, overflow takes place as shown in fig.6.

Between section I and II, a shock condition exists as

$$h_1(\mathbf{u}_1 - \boldsymbol{\omega}) - h_2(\mathbf{u}_2 - \boldsymbol{\omega}) = 0 \tag{27}$$

$$\mathbf{u}_{1}\mathbf{h}_{1}(\mathbf{u}_{1}-\omega)-\mathbf{u}_{2}\mathbf{h}_{2}(\mathbf{u}_{2}-\omega)=\frac{g}{2}\cdot(\mathbf{h}_{2}^{2}-\mathbf{h}_{1}^{2})$$
 (28)

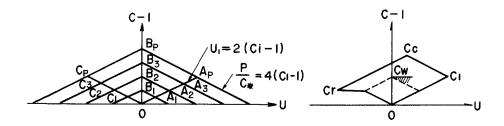


Fig 1 U-C characteristics of a long wave of finite amplitude.

Fig.2 Partial clapetis in U-C plane

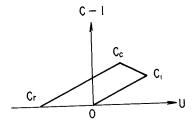


Fig.3 Partial clapotis in U-C plane when $C_{\mathbf{w}} = 1$

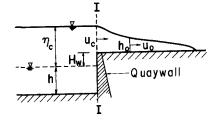


Fig. 4 Tsunamı transformation at the quaywall

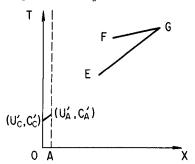


Fig.5 Characteristics at the brink of the quaywall and that of a leading front

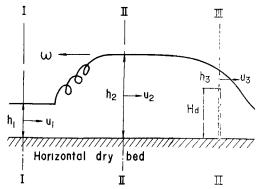


Fig.6 Reflection and overflow at a land dike

where ω is the speed of propagation of the bore front and suffix 1 and 2 refers to values in section I and II respectively.

Between section II and III, an energy equation holds as,

$$h_2 + \frac{u_2^2}{2g} = h_3 + \frac{u_3^2}{2g} + H_d$$
 (29)

and

$$u_2h_2=u_3h_3$$
 (30)

, in which ${\rm H}_{\rm d}$ is the height of the land dike and suffix 3 refers to values in section III. In section III, a critical condition is assumed as,

$$h_{3} = \sqrt[3]{\frac{(u_{3}h_{3})^{2}}{g}}$$
 (31)

From (27) and (28),

$$\omega = u_1 = \sqrt{\frac{gh_2}{2h_1} \cdot (h_1 + h_2)}$$
 (32)

as w is negative.

Putting eq. (32) into eq. (27), we get

$$u_{2} = (1 - \frac{Y}{F_{1}})u_{1} = \frac{Y}{F_{1}}u_{1}$$
 (33)

, where

$$Y=(x_2-1)\sqrt{1/2(1+\frac{1}{x_2})}$$
 , $x_2=\frac{h_2}{h_1}$. (34)

and

$$F_1 = \frac{u_1}{\sqrt{gh_1}}$$
, $y = F_1 - Y$ (35)

From (30) and (33)

$$x_3 = x_2^{2/3}$$
 . $(F_1 - Y)^{2/3} = (x_2 y)^{2/3}$ (36)

, where $x_3=h_3/h_1$

Putting (33) and (36) into (29), we get

$$z=x_2+1/2 y^2-3/2 (x_2y)^{2/3}$$
 (37)

, where

$$z = \frac{H_d}{h_1} \tag{38}$$

Fig.7 shows the relationship between \mathbf{x}_2 and \mathbf{F}_1 with a parameter \mathbf{z} and between \mathbf{z} and \mathbf{F}_1 with a parameter \mathbf{x}_2 . The height of reflected bore is nearly proportional to the Froude number of the incident flow. Also to keep \mathbf{x}_2 constant, \mathbf{z} must be lowered when \mathbf{F}_1 is increased. From eq. (33), overflow takes place when \mathbf{F}_1 is larger than \mathbf{Y} , which gives the lower limit of \mathbf{x}_2 as the latter is proportional to \mathbf{x} . This limit is designated as $\mathbf{x}_2(\mathbf{L})$ and is equal to the wall height \mathbf{z} as shown in eq. (37).

From eq. (32), the bore must be stopped resulting a hydraulic jump when $\omega = 0$, or

$$\mathbf{F}_{1}=\mathbf{x}_{2}\sqrt{\frac{1}{2}(1+\frac{1}{\mathbf{x}^{2}})}$$
 (39)

, which gives the higher limit of x_2 or $x_2(U)$ since the bore is flushed away when o. In this case the wall is no longer useful for a counter measure of the tsunami running flow. From (37),

$$\mathbf{z} = \mathbf{z}(\mathbf{U}) = \mathbf{x}_2(\mathbf{U}) + \frac{1}{2} (\frac{\mathbf{F}_1}{\mathbf{x}_2(\mathbf{U})})^2 - \frac{3}{2} (\mathbf{F}_1)^{2/3}$$
 (40)

in which z(U) means the wall height ratio for this limit case.

Eliminating x_2 from eq. (36) and (37), the relationship between x_3 and F_1 is given taking z as a parameter which is shown in fig.8. It is found that x_3 is almost linearly proportional to F_1 .

As shown in fig.9, flow runs still after overflowing the dike. Between section III and IV, following relations are hold, if energy loss is neglected.

$$h_3 + \frac{u_3^2}{2g} + H_d = h_4 + \frac{u_4^2}{2g}$$
 (41)

$$\mathbf{u}_{3}\mathbf{h}_{3}=\mathbf{u}_{4}\mathbf{h}_{4}\tag{42}$$

From eq. (41) and (42), the following equations is given together with eq. (31). $x_4^3 - (2 + \frac{3}{2} x_3) x_4^2 + \frac{1}{2} x_3^3 = 0$ (43)

in which
$$x_4 = h_4/h_1$$
. And
$$F_4 = \sqrt{\frac{u_4}{gh_4}} = (\frac{h_3}{h_4})^{3/2} = (\frac{x_3}{x_4})^{3/2}$$
 (44)

However it is convenient that x_4 is expressed as a function of F_1 taken z as a parameter, which is given in fig.10. It is shown that as z is higher, x_4 becomes smaller. Since at the front Froude number is between 1 and 2, height of land dikes is acceptable when it is designed by 0.4 < z < 2.2.

By difinition,

$$\frac{u_4}{u_1} = \frac{F_4}{F_1} \cdot x_4^{1/2} \tag{45}$$

$$\frac{q_4}{q_1} = \frac{F_4}{F_1} \cdot x_4^{3/2} \tag{46}$$

These are related to F_1 taking z as a parameter, in fig.11. As expected normally, invading flow decreases when the hight of a land dike increases. However velocity ratio increases causing stronger tractive force.

EXPERIMENTAL PROCEDURE

Experiments were conducted in a wave basin 23m long, 0.5m wide and 0.5m high. A pneumatic wave generator was installed at one end of the basin which dimension was 2.5m long, 1.5m wide and 1.5m high and was capable to produce a very long solitary wave. At the other end a horizontal dry bed model 10m long was installed which had a vertical quaywall of the height 0.312m.

Resistance type wave gauges were set 6m and 1m off the quaywall respectively. Fig.12 shows an example of recorded waves. Photographs of running water on the horizontal bed were taken by a motor driven camera and a 16mm movie camera at the rate of 3 frames and 24 frames per second respectively. Scales were marked on the bed and the wall, by which depth of wave front and water sheet were taken their co-ordinates using a profile-projector. Fig.13 and fig.14 show an example of wave fronts just after the quaywall and of waves overflowing the land dike respectively.

The depth of still water was set among 20 and 30cm. As a solitary wave, an incident wave element is expressed by

$$\gamma_{1}=H_{1} \operatorname{sech}^{2}\left(\frac{x}{h} \sqrt{\frac{3}{4} \frac{H_{1}}{h}}\right) \tag{47}$$

, where H_1 is the wave height of the solitary wave, in which 98% of total wave volume is included between ± 3.8 of x/h where the x origin is taken at the summit. So, for numerical calculation $_1$ is measured from the elevation at x/h= ± 5 . Then H_1 was chosen among 5 and 15cm. Also the period T is taken for the part of x/h= ± 5 in a wave, which was set among 4.7 and 28.5 sec. The height of land dikes was chosen between 3 and 12.5cm and these are located among 50 and 500cm from the quaywall.

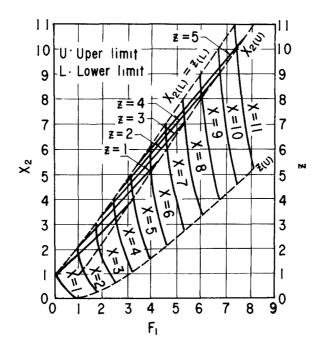
Total 426 runs were tested and several runs were compared with results of theoretical calculation.

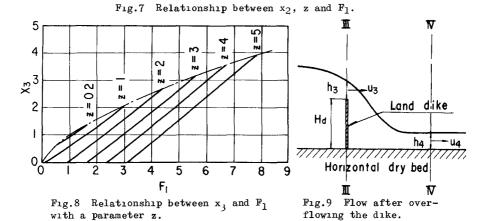
CALCULATION AND EXPERIMENTAL VERIFICATION

Using one of test conditions, following numerals are used for calculation.

$$h=28.1em, H_1=7.7em$$

The distance of a land dike from the quaywall Ld is 120 cm and its height





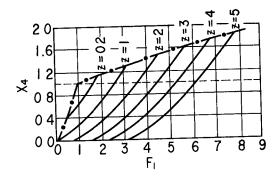


Fig.10 Relationship between \mathbf{x}_4 and \mathbf{F}_1 with a parameter z.

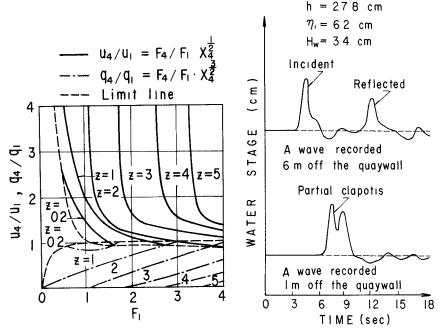


Fig.11 Relationship between u_4/u_1 , q_4/q_1 Fig.12 An example of and F1 with a parameter z.

recorded waves



Fig.13 A wave front just after the quaywall.



Fig.14 A wave over the land dike.

 H_d is 3.0 cm. Then from eq. (47)

$$_{1} = 7.7 \operatorname{sech}^{2}(0.453 \text{ x})$$
 (48)

, where X=x/h. In table 1, some specific values are given for points equally spaced on X-axis.

The height of a quaywall is taken as $\rm H_w=3.1cm$. U-C characteristics give values of the reflecting wave in table 2 following to the theory proposed. X-T and U-C characteristics are given in fig.15 and fig.16 respectively.

1.3		

Calculated point	(5)	(4),(6)	(3),(7)	(2),(8)	(1),(9)	(0),(10)
Х	0	1	2	3	4	5
η_1	7.7	6.314	3.717	1.789	0.782	0
$M_1 = \eta_1/h$	0.274	0.225	0.132	0.064	0.028	0
$C_1 = \sqrt{1+M_1}$	1.129	1.107	1.064	1.031	1.014	1
U ₁ =2(C ₁ -1)	0.257	0.213	0.128	0.063	0.028	0
$\left(\frac{dX}{dT}\right)_{+} = U_{1} + C_{1}$	1.386	1.320	1.192	1.094	1.041	1

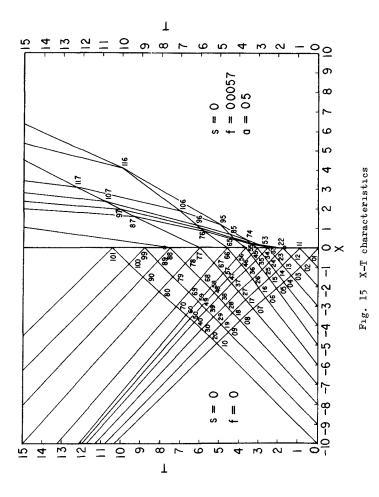
Table 2

Calculated point	(5)'	(4);(6)	(3);(7)	(2);(8)'	(1);(9)'	(0);(10)'
η_{r} (X=0)	1.532	1.532	1.532	1.532	0.783	0
$M_{f r}=\eta_{f r}/h$	0.05 5	0.055	0.055	0.055	0.028	0
$C_r = \sqrt{1+M_r}$	1.027	1.027	1.027	1.027	1.014	1
$U_{r}=-U_{1}$	-0.257	-0.213	-0.128	-0.063	-0.028	0
$(dX/dT)_{=U_r-C_r}$	-1.284	-1.240	-1.155	-1.090	-1.042	-1

Then values of surface elevation are given in table 3 and also are plotted in the left half of fig.17. It is cleary shown that the incident wave is transformed to the partial clapotis and is reflected at the quaywall.

Values of U and C at the quaywall just derived are converted to U' and C' by eq. (16) and $U_{\rm C}'=U_{\rm C}$. Then from eq. (17) $U_{\rm A}'$ and $C_{\rm A}'$ are calculated which gave boundary conditions for the overland flow. As shown in fig.16, the moment which the clapotis just touches the crest of the quaywall, is not coincided with an intersection of characteristics issuing from points given in table 1 and 2. So, assumption is made this moment is given by a fraction of time increment which is equal to that of U-C segment.

Then the first wave element emerges from (X=0, T=1.27 sec) on the X-T plane, from which a line of C_f characteristic is drawn by $dx/dt=U_A'+C_A'=2U_A'$ since $U_A'=C_A'$ as shown in eq.17. Moreover a line of front



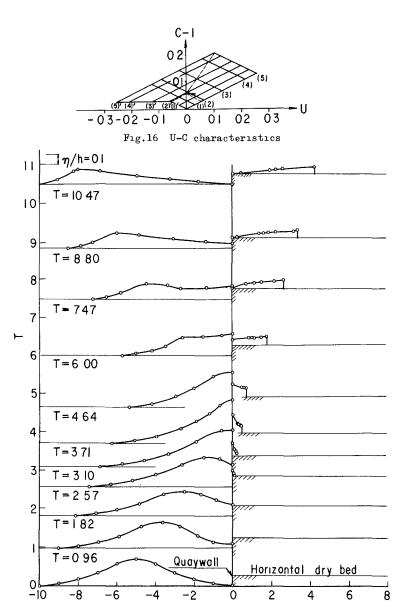


Fig.17 Calculated configuration of the tsunami overrunning the vertical quaywall.

Table 3

T==	x	0	-1	-2	- 3	-4	- 5	- 6	-7	- 8	- 9
0	η/h	0	0.028	0.064	0.132	0.225	0.274	0.225	0.132	0.064	0.028
T=	х	0	-1	-1.80	-2.74	-3.65	-4.73	-5.88	-6.97	- 8	-9.03
0.96	$\eta/_{ m h}$	0.053	0.064	0.132	0.225	0.274	0.225	0.132	0.064	0.028	0
T=	Х	0	-0.83	-1.64	-2.50	-3.59	-4.83	-6.00	-7.08	-8.16	
1.82	7 /h	0.124	0.164	0.228	0.274	0.225	0.132	0.064	0.028	0	
T=	Х	0	-0.67	-1.50	-2.62	-3.98	-5.20	-6.33	-7.45		
2.57	7 /h	0.231	0.295	0.309	0.225	0.132	0.064	0.028	0		
T=	х	0	-0.58	-1. 90	-3.32	-4.62	-5.75	-6.90			
3.10	7 /h	0.374	0.371	0.263	0.132	0.064	0.028	0			
T=	Х	0	-0.65	-1.20	-1.87	-2. 68	- 3.95	-5.1 1	-6.27		
3.71	$\eta/_{ m h}$	0.454	0.395	0.313	0.234	0.153	0.064	0.028	0		
T=	Х	0	-1.03	-2.03	-2.03	-2.95	-4.20	-5.39			
4.64	7 /h	0.374	0.329	0.199	0.115	0.030	0				
T=	Х	0	-1.53	-2.60	-3.50	-4.21	-5.00	-5.7 6			
6.00	$\eta_{ m /h}$	0.231	0.201	0.193	0.103	0.055	0.026	0			
T=	Х	0	-1.35	-2.70	-3.37	-4.47	-5. 82	-6. 55	-7. 25		
7.47	η/h	0.124	0.115	0.111	0.136	0.160	0.055	0.026	0		
T=	Х	0	-1.40	-3.07	-4.86	-6.00	-7. 25	-7. 90	- 8.53		
8.80	η/h	0.053	0.061	0.092	0.136	-0160	-0055	0.026	0		
T=	х	0	-1.78	-3.22	-4.95	-6. 82	-8.00	-8.26	-9.0 8	-10.15	,
10.47	$\eta_{ m /h}$	0	0.026	0.057	0.092	0.136	0.160	0.136	0.055	0	

characteristics is drawn also by

$$\frac{dx}{dT} = \sqrt{U_A^{'2} - \frac{2f}{a^2} \cdot \frac{X - X_a}{(1 + a)(1 + 2a)}}$$
 (49)

in which a and f are given as 1/2 and 0.0057 respectively. In the right half of fig.15, X-T characteristics are obtained and in table 4 values of 7/h are given. Also in the right half of fig.17, calculated values of surface elevation are plotted. Fig.18 shows the heighest traces of incident, reflected and run-up waves. Agreement between results of experiment and of calculation is fine. Fig.19 shows the relationship between

 $\frac{C_c-1}{C_w-1}$ and $\frac{C_1-1}{C_w-1}$, where a full line shows the relationship given by eq. (4)

Table 4

	Х	0	0.03	0.05	0.08				
T=2.57		ſ			-				
	η/h	0.059	0.034	0.029	0.003				
T=3.10	Х	0	0.09	0.16	0.21				
	η/h	0.136	0.070	0.053	0.032				
T=3.71	X	0	0.23	0.30	0.42	0.45			
1=3.11	η/h	0.181	0.098	0.092	0.077	0.074			
m 4 64	Х	0	0.47	0.58	0.69	0.98			
T=4.64	η/h	0.136	0.102	0.097	0.099				
T=6.00	Х	0	0.82	1.00	1.11	1.48	1.77		
1=0.00	η/h	0.059	0.081	0.080	0.081	0.086	0.097		
T=7.47	X	0	0.70	1.13	1.50	2.15	2.65		
1=7.47	η/h	0.006	0.050	0.059	0.068	0.074	0.093		
T=8.80	Х	0	0.21	1.35	1.60	1.83	2.25	3.18	3.37
	η/h	0	0.006	0.044	0.048	0.053	0.062	0.067	0.088
T=10.47	Х	0	0.45	1.98	2.23	2.61	4.27		
	η/h	0	0.006	0.037	0.041	0.051	0.067		

and white circles show experimental results. Agreement is also very fine which proves the assumption for the formation of imperfect clapotis. In fig.20, the front characteristics in X-T plane is presented to compare test results and theoretical ones, which were obtained by assuming f as 0.0057 and 0.01. It is concluded that a frictional coefficient must be taken much larger than that ordinary expected.

The Froude number of the wave front was calculated for nearly 80 runs and was found among 0.5 and 2.5 which might correspond to 1.0 and 2.0 given by Abbottand Méhauté.

Finally, test results of x₃ and $F_4=u_4/\sqrt{gh_4}$ are compared with theretical ones in fig.21 and fig.22 respectively, which also show good agreement with each other.

CONCLUSION

U-C characteristics are utilized to analyse perfect and imperfect reflection at the quaywall. Condition of occurance of imperfect clapotis is presented. No dimensional wave celerity and velocity are given by eq. (4) and (5).

Overland flow is calculated assuming that critical flow takes place at the quaywall and Froude number $F_1=U_{\tilde{P}}/C_{\tilde{f}}=1/a$ on the leading wave front is 2. However whenever this front is took over by the succeeding elements, abrupt change is occurred in U' and C'.

Reflection and overflow of running tsunami at a land dike which is designed to prevent the intrusion of tsunami are analysed using shock

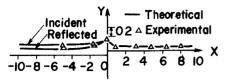


Fig.18 Max. traces of incident, reflected and inundated waves.

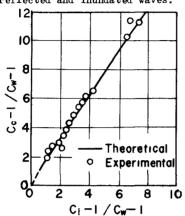


Fig.19 Relationship between C_c-1/C_w-1 and C_1-1/C_w-1 .

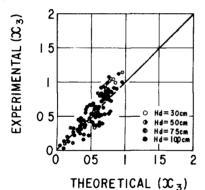


Fig.21 Comparison between theoretical and experimental values of x_3 .

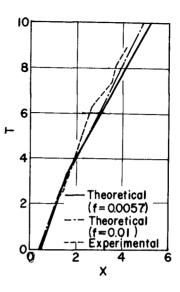


Fig.20 X-T characteristics of the tsunami front on the land.

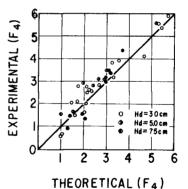


Fig.22 Comparison between theoretical and experimental values of F_4 .

condition and an energy equation, in which also the critical depth is assumed to occure at the summit of the dike.

Conditions of perfect reflection and of jet impact are given. Also depth, velocity and discharge behind the dike after overflow are presented. It is found that as the height of a dike increases, overflow discharge decreases as expected ordinary, but velocity increases which necessitates careful inspection on safety of the land behind the dike.

Finally theories are examined by experiments of 426 runs and are verified by comparison of test results and theoretical calculations.

ACKNOWLEDGEMENTS

Authors wish to express their thanks to Messrs. W. Taniguchi, S. Noji, K. Hashimoto and T. Murayama of undergraduate students of Tohoku University for their excellent achievement on experiments and calculations.

REFERENCES

- M.B. Abbott: On the Spreading of One Fluid over Another. La Houille Blanche, Decembre 1961 N 6, pp 827-836
- 2) J.C. Freeman and LeMéhauté B.L.: Wave Brakers on a Beach and Surges on a Dry Bed.
 - Proc. ASCE. Vol. 90 No.HY2 1964, pp 187-216
- 3) Lamb, H: Hydrodynamics, 6th edition Cambridge 1932. p.279